



Estimation of Subsurface Structure based on Microtremor and Gravity Survey in the Shikano Area, Tottori Prefecture, Japan

T. Noguchi⁽¹⁾, T. Kagawa⁽²⁾, S. Yoshida⁽³⁾, H. Ueno⁽⁴⁾

⁽¹⁾ Assistant Professor, Tottori University, noguchit@cv.tottori-u.ac.jp

⁽²⁾ Professor, Tottori University, kagawa@cv.tottori-u.ac.jp

⁽³⁾ Graduate Student, Tottori University, D16T4003B@edu.tottori-u.ac.jp

⁽⁴⁾ Graduate Student, Tottori University, M16T6005U@edu.tottori-u.ac.jp

Abstract

Shikano and Yoshioka earthquake fault occurred on the surface by the 1943 Tottori earthquake. In this study, subsurface structures were determined and we grasped characteristics of ground motion by microtremor and gravity survey in the Shikano area, Tottori Prefecture. Microtremor single-point 3-components observations and array observations were carried out at 304 and 34 sites respectively. As analysis of microtremor surveys data, we estimated S-wave velocity structures by using phase velocities obtained from array observations and predominant periods of H/V spectrum obtained from single-point 3-components observation records. Gravity observations were carried out at 38 sites. As analysis of gravity surveys data, gravity anomalies with assumed density in 2.4g/cm^3 were obtained by using gravity databases, existing data in the east-part of Tottori Prefecture and this study data. 3D density structures from the distribution of gravity anomalies were estimated. We simulated strong ground motions at 3 seismic stations where subsurface structures are different. Then we could evaluate difference of characteristics of seismic ground motion.

Keywords: microtremor survey, gravity survey, subsurface structure, Shikano fault

1. Introduction

The target area of this study is the Shikano area, Tottori Prefecture, Japan. Damaging earthquakes; the 1943 Tottori earthquake and the 2000 Western Tottori prefecture earthquake occurred in the area. The severely damaged area was concentrated on some parts of the plains and Shikano and Yoshioka earthquake fault occurred on the surface by the 1943 Tottori earthquake [1]. It is thought that this concentration of damage was caused by the characteristics of the strong earthquake motion, which is given by the local site effects of the area. We need to investigate the causes of the local site effects for the prevention or mitigation of earthquake disasters in the area. In this study, subsurface structures were estimated and we grasped characteristics of ground motion by microtremor and gravity survey in the Shikano area, Tottori Prefecture.

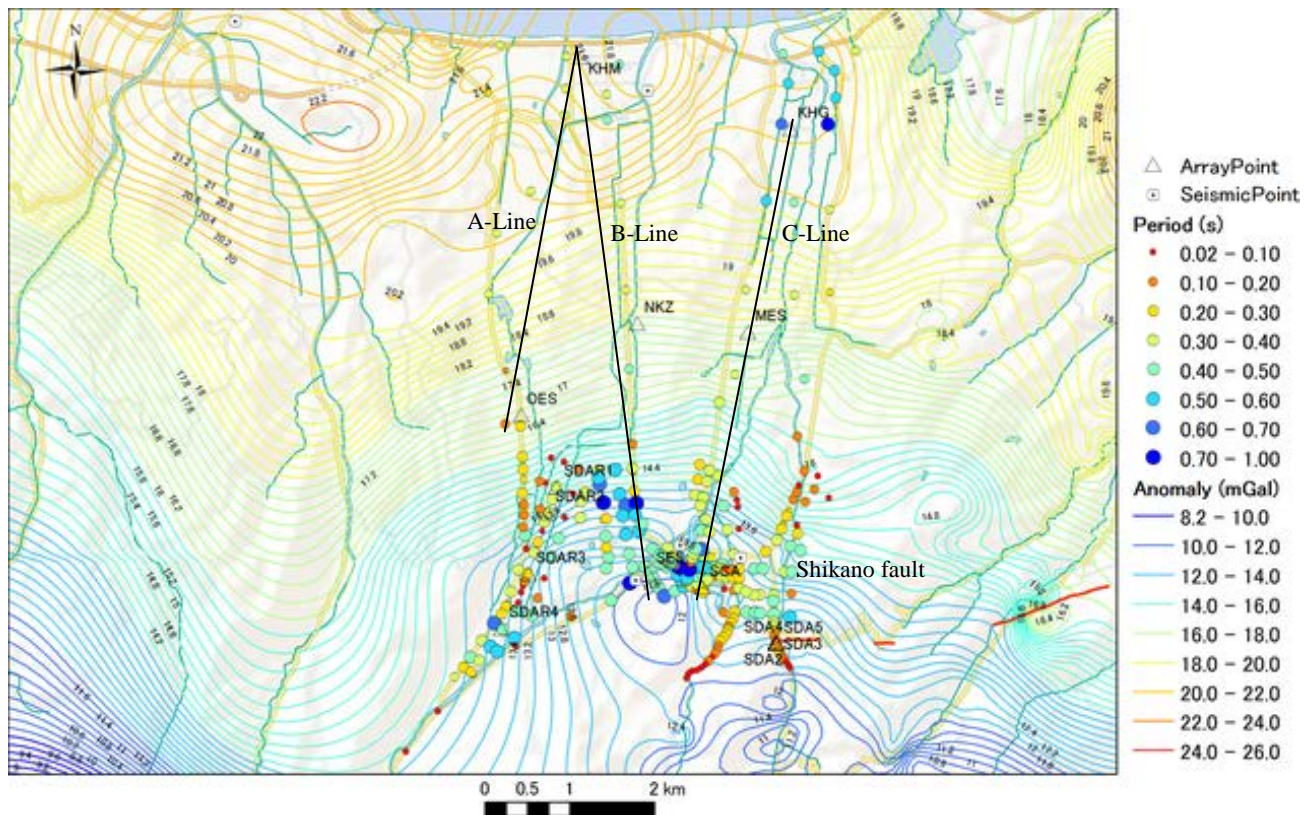


Fig. 1 – Distribution of predominant period and contour map of gravity anomaly (whole area)

2. Survey and analysis

2.1 Microtremor survey and analysis

3-component single-site observations at 304 points and array observations at 37 sites were made to observe microtremor in the area. The array observation was executed by using many kinds of radii within the range from 0.6m to be 600m for each site according to the situation of the site. The 3-component single-site and small array observation (radius: 0.6m-15m) carried out about 20 - 50m interval in a Shikano-town city area and the Shikano earthquake fault area densely. The 3-component single-site observation (100m-500m interval) and array observation (radius: 0.6m-600m) were carried out in Shikano-town city area regionally.

For the analysis of the 3-component single-site observation data, portions of 20.48s without artificial noise were selected from the array observation records. A horizontal-to-vertical spectral ratio (H/V spectrum) was calculated by using the averaged each component Fourier spectra of the selected data. Horizontal components

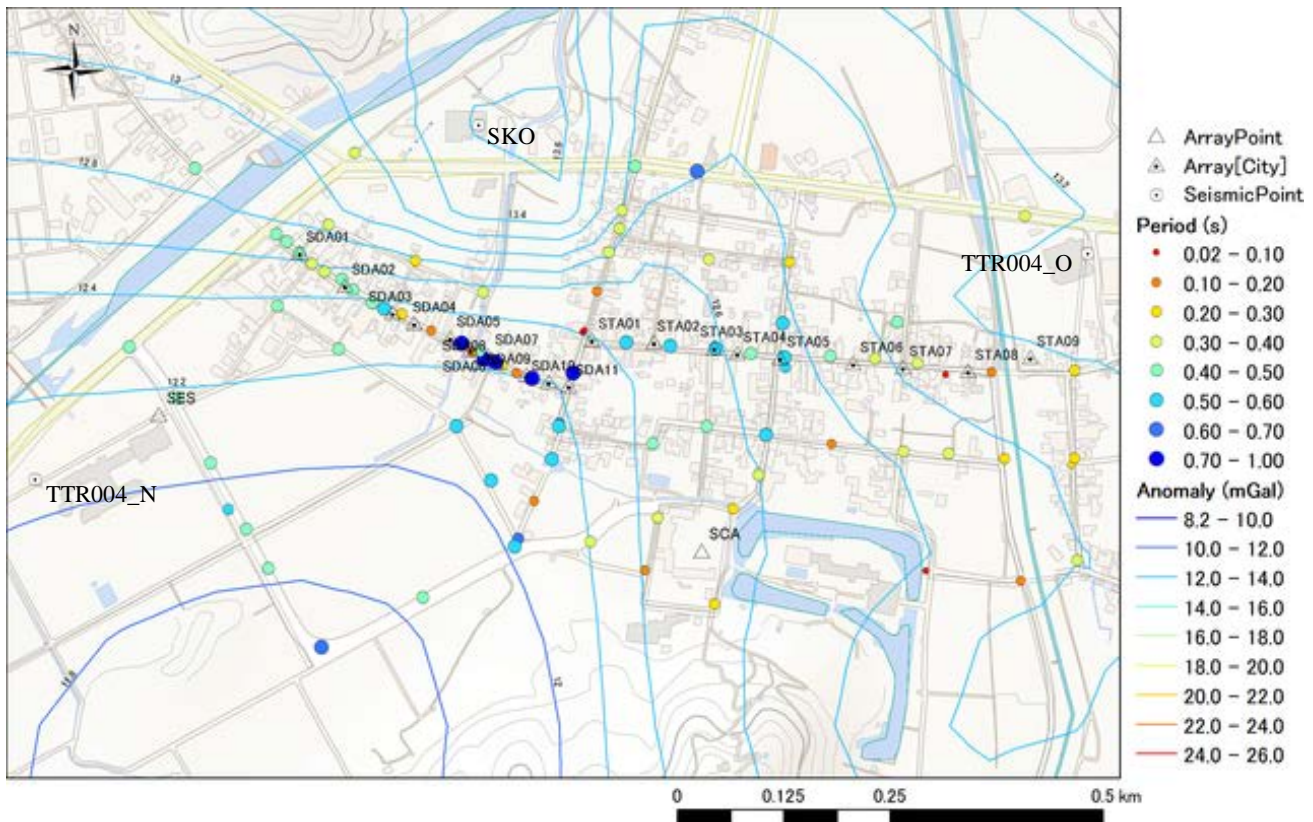


Fig.2 – Distribution of predominant period and contour map of gravity anomaly (city area)

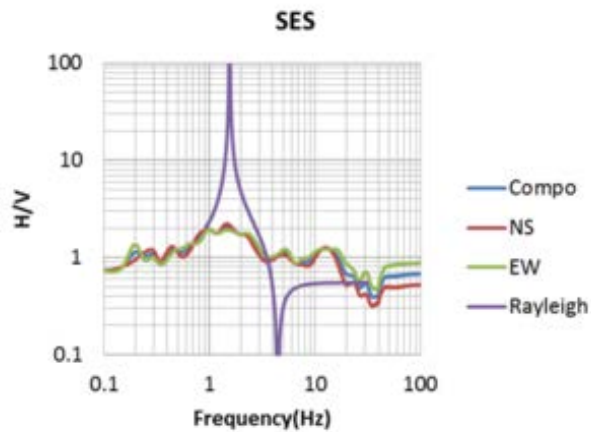


Fig.3 – H/V spectra (SES)

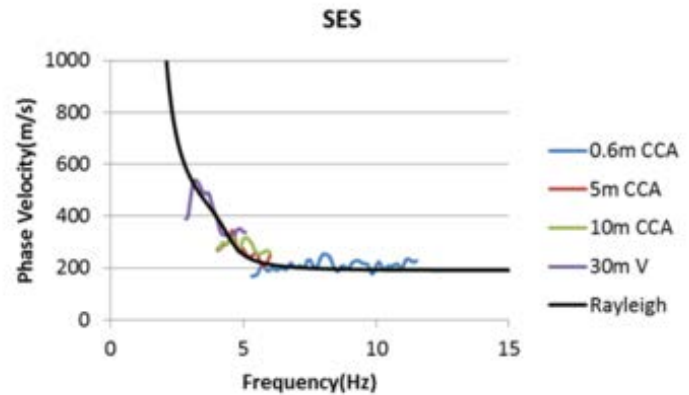


Fig.4 – Dispersion curves of phase velocity (SES)

were composed. Spectra were smoothed by a Log-window [2] with coefficient of 20. Predominant periods of H/V each sites were read and a distribution map of predominant periods was made by using interpolation of spline function. The distribution maps of predominant periods of H/V spectra in a whole area and a city area are shown in Fig. 1 and Fig. 2 respectively. H/V spectra of center point of array at the SES is shown in Fig. 3.

For the analysis of the array observation data, CCA [3], nc-CCA [4], V [4], SPAC [5] method are applied and phase velocities are estimated. The CCA, nc-CCA, V, SPAC method are techniques of geophysical exploration that is used to infer phase velocities of surface waves using records of microtremor from a circular array of seismic sensors deployed on the ground surface. The frequency range of the dispersion curves of phase velocity are 2Hz-40Hz. The minimum and maximum values of phase velocity are 100m/s and 1600m/s, respectively. Dispersion curves of phase velocity at the SES are shown in Fig.4. The velocity structures



Table 1– Subsurface structure models

KHM				KHG				OES			
Thickness (m)	ρ (g/cm ³)	Vp(m/s)	Vs(m/s)	Thickness (m)	ρ (g/cm ³)	Vp(m/s)	Vs(m/s)	Thickness (m)	ρ (g/cm ³)	Vp(m/s)	Vs(m/s)
17	1.9	1515	200	18	1.6	1405	100	5	1.6	1435	130
15	2.0	1845	500	30	2.1	2180	800	15	2.0	1845	500
40	2.1	2180	800	100	2.2	2955	1500	40	2.1	2180	800
100	2.2	2955	1500	∞	2.3	4065	2500	100	2.2	2955	1500
∞	2.3	4065	2500					∞	2.3	4065	2500

SES				NKZ				MES			
Thickness (m)	ρ (g/cm ³)	Vp(m/s)	Vs(m/s)	Thickness (m)	ρ (g/cm ³)	Vp(m/s)	Vs(m/s)	Thickness (m)	ρ (g/cm ³)	Vp(m/s)	Vs(m/s)
20.7	1.9	1515	200	3	1.6	1435	130	4.1	1.6	1470	160
21	2.0	1845	500	8	2.0	1625	300	10.8	2.0	1570	250
35	2.1	2180	800	30	2.1	2180	800	30	2.1	2180	800
100	2.2	2955	1500	100	2.2	2955	1500	100	2.2	2955	1500
∞	2.3	4065	2500	∞	2.3	4065	2500	∞	2.3	4065	2500

SCA				SDAR1				SDAR2			
Thickness (m)	ρ (g/cm ³)	Vp(m/s)	Vs(m/s)	Thickness (m)	ρ (g/cm ³)	Vp(m/s)	Vs(m/s)	Thickness (m)	ρ (g/cm ³)	Vp(m/s)	Vs(m/s)
3.2	1.8	1435	130	3	1.8	1460	150	3.8	1.8	1490	180
60	2.1	2180	800	10	2.0	1850	500	12	1.9	1850	500
100	2.2	2955	1500	30	2.1	2070	700	40	2.0	2070	700
∞	2.3	4065	2500	300	2.3	2620	1200	300	2.2	2620	1200
				∞	2.5	3620	2100	∞	2.4	3620	2100

SDAR3				SDAR4			
Thickness (m)	ρ (g/cm ³)	Vp(m/s)	Vs(m/s)	Thickness (m)	ρ (g/cm ³)	Vp(m/s)	Vs(m/s)
4	1.8	1520	210	5	1.8	1560	240
18	2.0	1850	500	25	2.0	1730	500
40	2.1	2070	700	65	2.2	2070	700
300	2.3	2620	1200	300	2.4	2620	1200
∞	2.5	3620	2100	∞	2.6	3620	2100

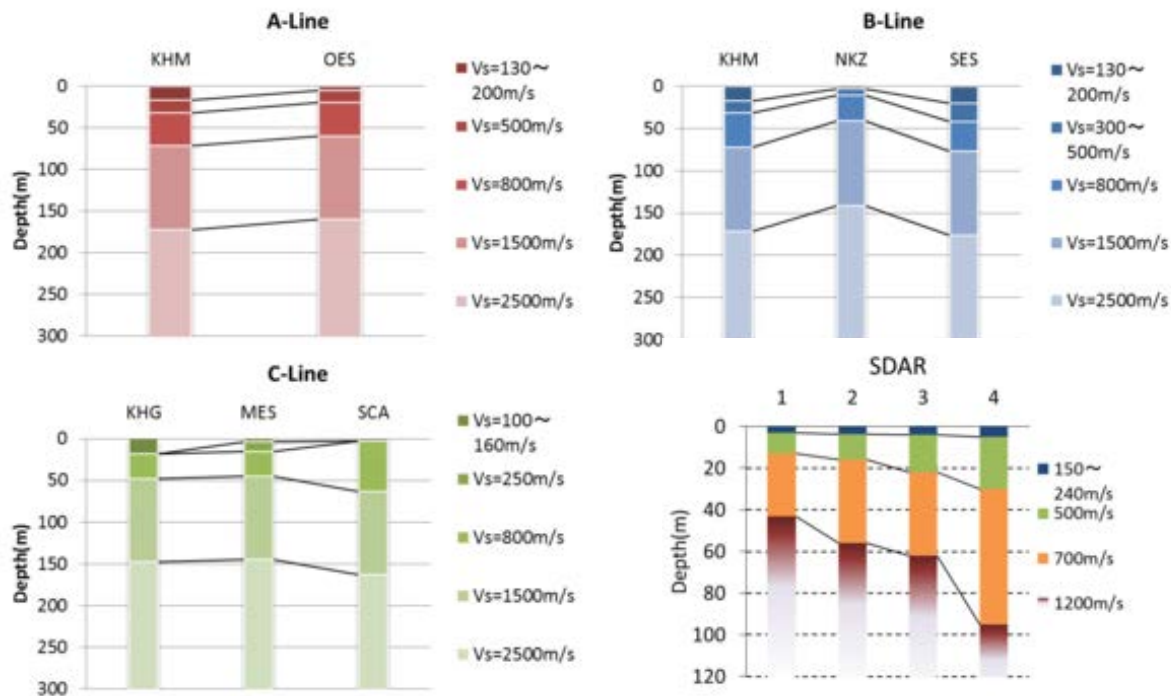


Fig.5 – Columnar sections of S-wave velocity structure

were determined by using a heuristic approach based on forward calculation. We determined to satisfy the phase velocity and the H/V by using fundamental mode of Rayleigh wave in the frequency range of 2 - 40Hz. Parameters of the subsurface structure models are number of layers, density, P-wave velocity; Vp, S-wave velocity; Vs and layers thickness.

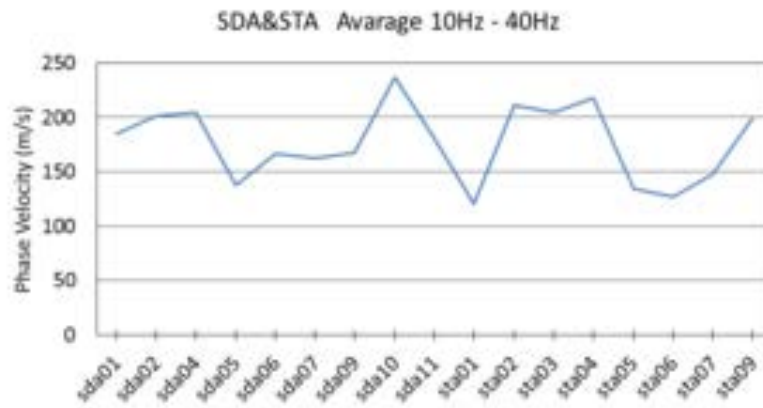


Fig.6 –Distribution of averaged phase velocity (SDA, STA)

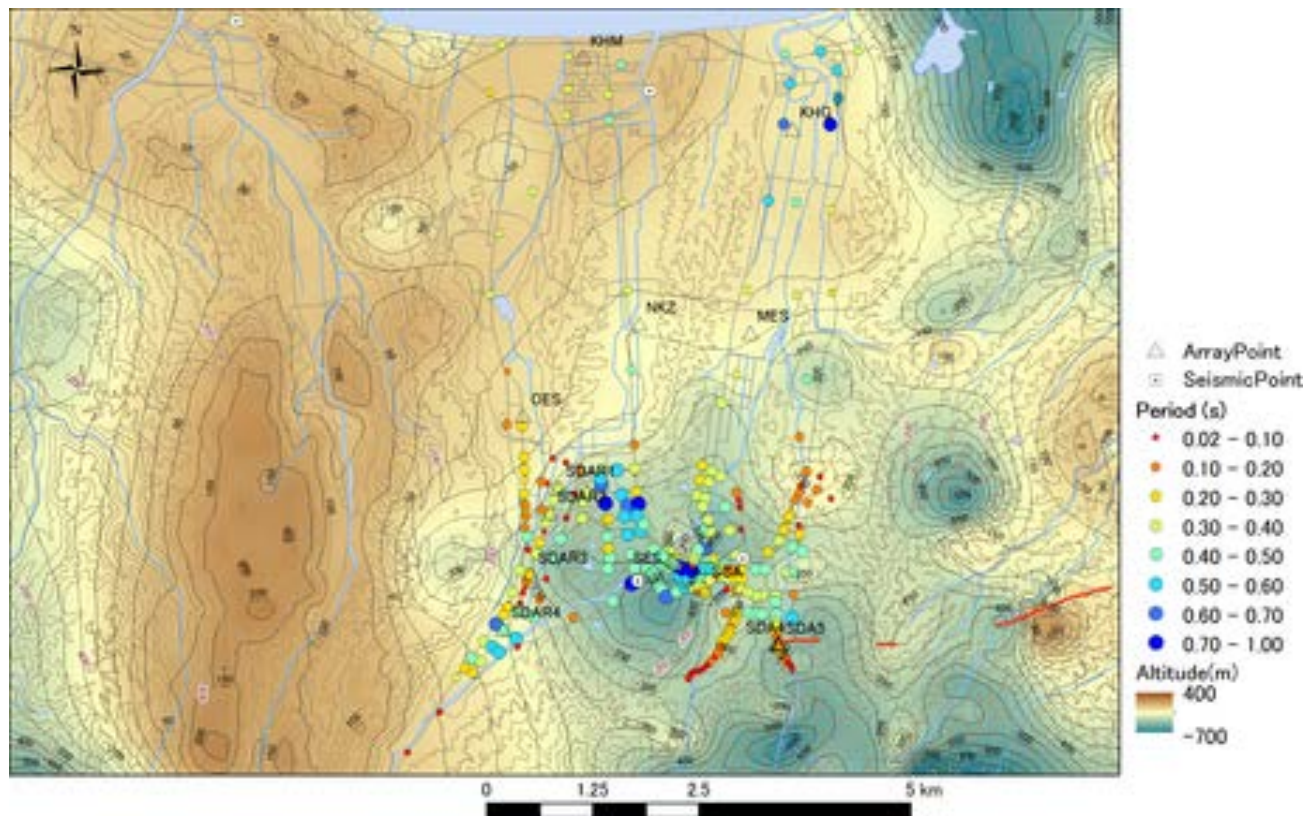


Fig.7 – A Contour map of 3D gravity basement with distribution of predominant period

2.2 Gravity survey

The gravity survey was carried out at about 500m - 1km intervals at 38 sites in the area and published data from gravity database CD-ROM [6], [7]. A Lacoste-Lon-Berg G-type gravimeter was used. The precision of the elevation measurements was kept within 1m by using VRS-GPS or differential GPS survey systems. The terrain correlation was made with a topographic 50 m and 250 m mesh digital data to obtain the gravity anomaly. An adequate setting of the densities is vital to estimate the subsurface profile appropriately. A suitable assumed density of gravity anomaly was determined to be 2.43g/cm^3 as a bedrock layer. Contour maps of gravity anomaly in the whole area and city area are shown in Fig.1 and Fig.2 respectively.

Program codes of a 3D analysis method [8] were used to determine 3D density structures. This method uses the automatic forwarding method of underground structure. The parameters required are density differences

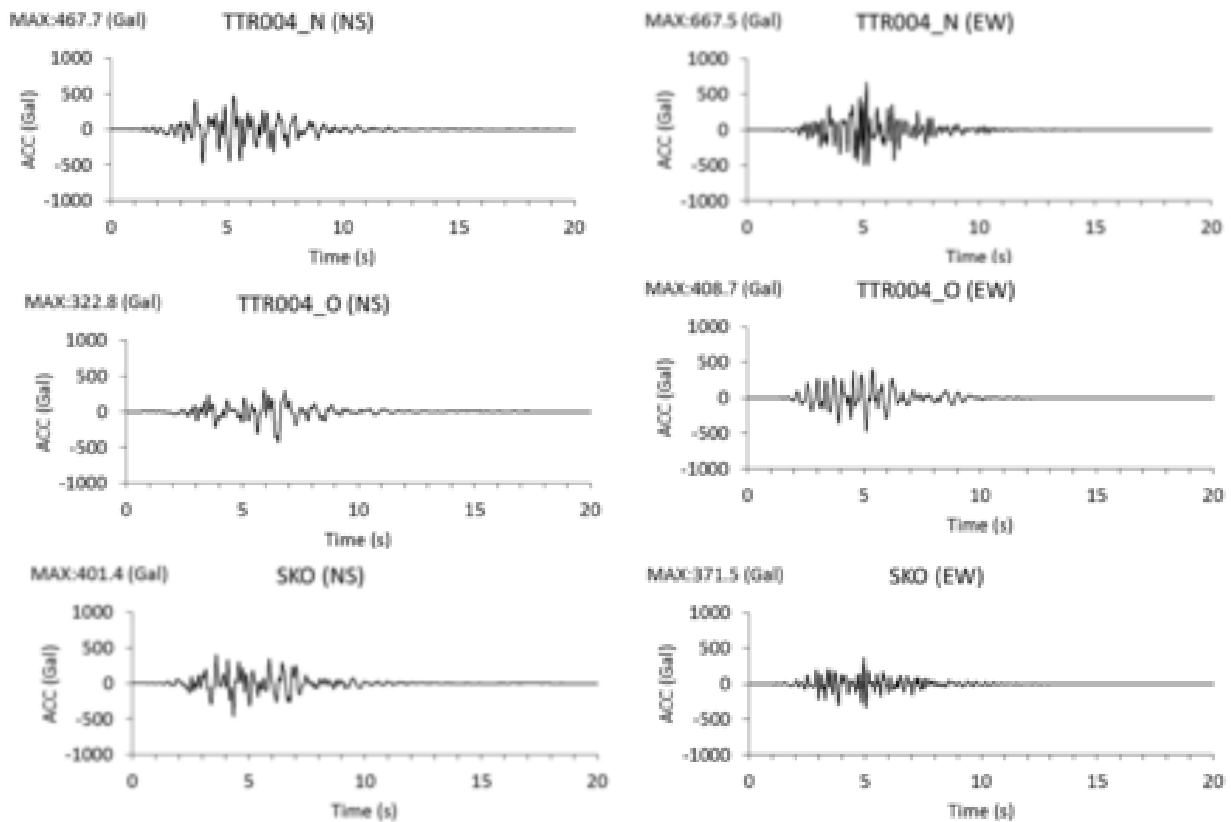


Fig.8 – Simulated acceleration waves (horizontal components)

between surface and bedrock layers of two homogeneous layers and a control point for bedrock depth. In addition, the depth to the bedrock layer in the 2-layer model was restricted to the outcrop point. We thought the density difference between the sediments and the bedrock layers was optimized to be 0.23 g/cm^3 in the case of 2-layer model. To remove the effect of the deep structure, a band pass filter that combines two upward continuation filters of 50 m and 3000 m was used.

3. Subsurface structure

3.1 Results of microtremor data analysis

From the distribution maps of predominant periods of H/V spectra in the whole area (Fig.1), it is found that long period (longer than 0.5 seconds) area is distributed around SCE in the city area and around KHG in a coastal area. From the distribution maps in the city area (Fig.2), the long period area is concentrated at the central city area. We consider that a different of subsurface structure influences the characteristics of the distribution.

The layers with some different velocities structure were determined from the array observation data at each site. The final subsurface structure models of 11 sites are shown in Table 1 and columnar sections of S-wave velocity structure (indicated the location of lines on Fig.1) are shown in Fig.5. It is found that a basement depth to boundaries of layers become shallow between at a coast and an inland site from Fig.5. The results of another area where on an extension line of the Shikano earthquake fault (indicated the location on Fig.1; SDAR1-4) is shown in Table 1 and Fig.5. It is found that the depths to boundaries of layers are deepened from No.1 to No.4. Especially, there is great change between No.3 and No.4 on the extension line of Shikano earthquake fault. The results of mini-array (array radius is 0.6m) observation at 20 site (indicated the location on Fig.3; SDA01-11 and STA01-09) in the city area are shown in Fig.6. This figure was shown values that averaged phase velocity in the range of 10Hz-40Hz in the SDA and STA line. It is found that phase velocity is low in sda05-sda09, sta01 and sta05-sta07 from Fig.6.

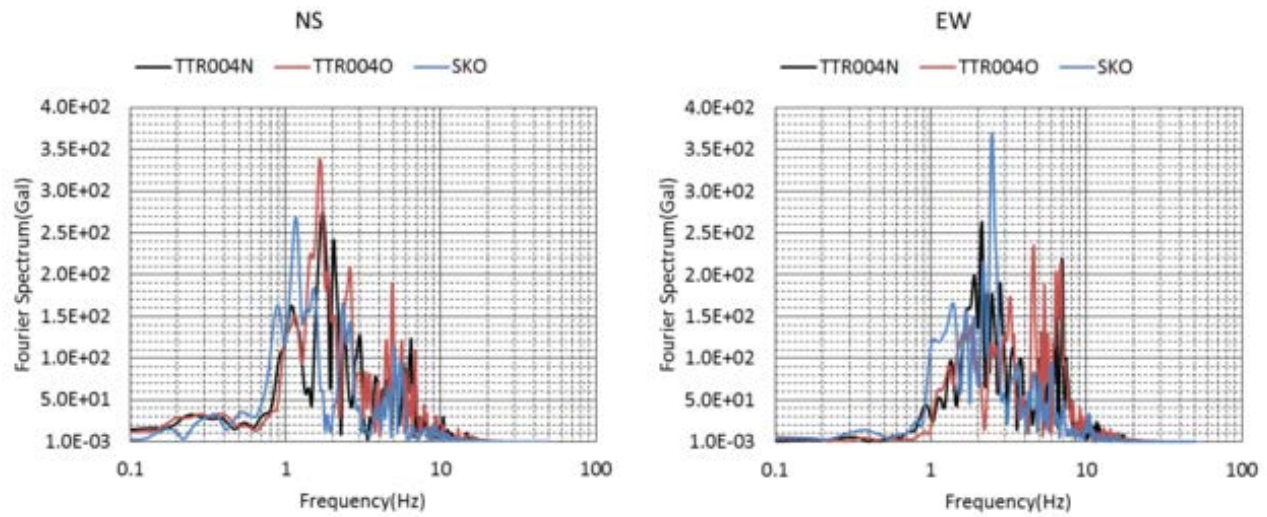


Fig.9 – Fourier spectra of simulated waves

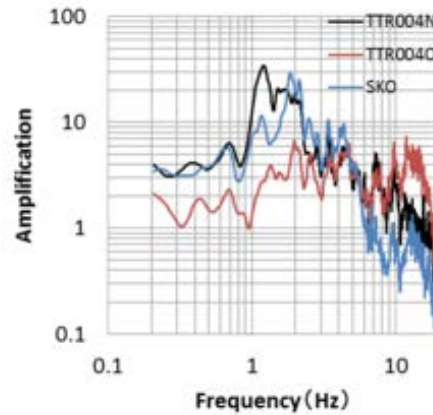


Fig.10 – Characteristics of amplification factors

3.1 Results of gravity data analysis

An overview of the distribution of gravity anomaly (Fig.1) as follows. Low anomaly areas are found in a southern part, Shikano-town city area. In contrast, high anomaly areas are found in a northern part and coastal area. Low anomaly areas are located in the area where predominant period of H/V is long. We consider that these anomalies are caused by a difference of a mountain rock density or a depth to basement rock.

The 3D density structure was automatically calculated from the gravity anomaly at chapter 2.2. The 3D bedrock structure is shown in Fig.7. An overview of 3D bedrock structure is as follows. Deep bedrock areas whose depth is approximately 200m-500m are found in the southern part, Shikano-town area and mountain area. Shallow area whose depth to bedrock is approximately less than 0m is found in the northern part, coast area. The maximum depth to bedrock is approximately 600m.

4. Site amplification effects

On September 10, 1943, the Tottori earthquake occurred in the east of Tottori prefecture, and generated serious damage in the eastern Tottori Prefecture. Then we evaluated strong ground motion of the seismic basement of the Tottori earthquake at 3 seismic observation sites; TTR004_N (K-NET Shikano; new station), TTR004_O (K-NET Shikano; old station), SKO (Shikano-town office) shown in Fig.3. Strong ground motions (horizontal components) were simulated using stochastic Green's function observation station on method [9] for element



earthquake, empirical Green's function method [10] for synthesizing earthquake and the characterized source model [11]. Engineering basement waves and surface waves were calculated using Haskell matrix [12] and SHAKE [13] respectively. The subsurface structure models that we have decided in this study were used to calculate surface waves. The calculated acceleration waves and these Fourier spectra are shown in Fig.8 and Fig.9 respectively. In addition, the characteristics of amplification factors [14] are shown in Fig.10. The results are as follows. TTR004_N of the peak ground acceleration is the largest in these sites. The Fourier spectrum shapes of TTR_N and SKO are similar and larger than TTR_O in the range of 0.2Hz - 2Hz. The characteristics of amplification factors are same situation as the Fourier spectrum. We consider that a different of subsurface structure influences the ground strong motion.

5. Conclusion

The subsurface structures were determined and we grasped characteristics of ground motion by microtremor and gravity survey in the Shikano area, Tottori Prefecture. The analysis of microtremor surveys data, we estimated S-wave velocity structures and predominant periods of H/V spectrum. The analysis of gravity surveys data, gravity anomalies with assumed density in 2.4g/cm^3 were obtained by using gravity databases, existing data in the east-part of Tottori Prefecture and this study data. 3D density structures from the distribution of gravity anomalies were estimated. We simulated strong ground motions at 3 seismic stations where subsurface structures are different. Then we could evaluate difference of characteristics of seismic ground motion at each site.

6. Acknowledgements

We used borehole data of the National Research Institute for Earth Science and Disaster Prevention (NIED) for calculating the strong ground motion.

7. References

- [1] Architectural Institute of Japan (1994): The Tottori prefecture earthquake disaster investigation report, *Jour. of Architecture and Building Science* (in Japanese).
- [2] Konno, K. and T. Ohmachi (1995): A smoothing function suitable for estimation of amplification factor of the surface ground from microtremor and its application, *Journal of JSCE*, No.524/1-33, 247-259 (in Japanese).
- [3] Cho, I., T. Tada, and Y. Shinozaki (2006): Centerless circular array method: Inferring phase velocities of Rayleigh waves in broad wavelength ranges using microtremor records, *J. Geophys. Res.*, 111, B09315.
- [4] Tada, T., I. Cho, and Y. Shinozaki (2007): Beyond the SPAC method: exploiting the wealth of circular-array methods for microtremor exploration, *Bull. Seism. Soc. Am.*, 97, 2080-2095.
- [5] Aki, K. (1957): Space and time spectra of stationary stochastic waves, with special reference to microtremors, *Bull. Earthq. Res. Inst.*, 35, pp.415-456.
- [6] The Gravity Research Group in Southwest Japan (Representatives: Ryuichi Shichi and Akihiko Yamamoto) (2001): Gravity Measurements and Database in Southwest Japan, Gravity Database of Southwest Japan (CD-ROM), *Bull. Nagoya University Museum*, Special Rept., No.9.
- [7] Komazawa, M. (2013): Gravity Grid Data of Japan, Gravity Database of Japan, DVD edition, *Digital Geoscience Map P-2*, Geological Survey of Japan, AIST.
- [8] Komazawa, M. (1995): Gravimetric analysis of volcano and its interpretation, *Jour. Geod. Soc. Japan*, 41; 1; 17-45.
- [9] Boore, D. M. (1983): Stochastic Simulation of High-frequency Ground Motions Based on Seismological Models of the Radiation Spectra, *Bull. Seism. Soc. Am.*, 73, pp. 1865-1894.
- [10] Irikura, K. (1986): Prediction of strong acceleration motion using empirical Green's function, *7th Jpn. Earthq. Eng. Symp.*, pp.151-156.



- [11] Yoshida, S., T. Noguchi and K. Kagawa (2016): Estimation of subsurface structure from microtremor observation and strong motion evaluation at school damage sites due to the 1943 Tottori Earthquake, *Journal of Earthquake Engineering, JSCE*, Vo.72, No.4 (in Japanese) [in press].
- [12] Haskell, N. A. (1953): The dispersion of surface waves on multilayered media, *Bull. Seism. Soc. Am.*, 43, pp. 17-34.
- [13] Schnabel, P. B., J. Lysmer and H. B. Seed. (1975): SHAKE a computer program for earthquake response analysis of horizontally layered sites, *University of California, Berkeley, Report*, No. EERC72-12, 1975.
- [14] Noguchi, T., H. Nishikawa, S. Yoshida and T. Kagawa (2016): Subsurface structure and evaluation of site effects at strong ground motion observation sites in Tottori prefecture, *Journal of Earthquake Engineering, JSCE*, Vo.72, No.4 (in Japanese) [in press].